New Olenekian austrolimulid from Russia uncovers role of Triassic horseshoe crabs as disaster taxa (#59506)

First submission

Guidance from your Editor

Please submit by **29 Apr 2021** for the benefit of the authors (and your $200 publishing discount) .

Structure and Criteria
Please read the 'Structure and Criteria' page for general guidance.

Custom checks
Make sure you include the custom checks shown below, in your review.

Author notes
Have you read the author notes on the guidance page?

Raw data check
Review the raw data.

Image check
Check that figures and images have not been inappropriately manipulated.

Privacy reminder: If uploading an annotated PDF, remove identifiable information to remain anonymous.

Files

Download and review all files from the materials page.

10 Figure file(s)
4 Raw data file(s)

Custom checks

New species checks

- Have you checked our new species policies?
- Do you agree that it is a new species?
- Is it correctly described e.g. meets ICZN standard?

Structure and Criteria

Structure your review

The review form is divided into 5 sections. Please consider these when composing your review:

1. **BASIC REPORTING**
2. **EXPERIMENTAL DESIGN**
3. **VALIDITY OF THE FINDINGS**
4. General comments
5. Confidential notes to the editor

You can also annotate this PDF and upload it as part of your review

When ready submit online.

Editorial Criteria

Use these criteria points to structure your review. The full detailed editorial criteria is on your guidance page.

BASIC REPORTING

- Clear, unambiguous, professional English language used throughout.
- Intro & background to show context. Literature well referenced & relevant.
- Structure conforms to PeerJ standards, discipline norm, or improved for clarity.
- Figures are relevant, high quality, well labelled & described.
- Raw data supplied (see PeerJ policy).

EXPERIMENTAL DESIGN

- Original primary research within Scope of the journal.
- Research question well defined, relevant & meaningful. It is stated how the research fills an identified knowledge gap.
- Rigorous investigation performed to a high technical & ethical standard.
- Methods described with sufficient detail & information to replicate.

VALIDITY OF THE FINDINGS

- Impact and novelty not assessed. Negative/inconclusive results accepted. *Meaningful* replication encouraged where rationale & benefit to literature is clearly stated.
- All underlying data have been provided; they are robust, statistically sound, & controlled.
- Speculation is welcome, but should be identified as such.
- Conclusions are well stated, linked to original research question & limited to supporting results.

Standout reviewing tips

The best reviewers use these techniques

Tip	*Example*
Support criticisms with evidence from the text or from other sources	*Smith et al (J of Methodology, 2005, V3, pp 123) have shown that the analysis you use in Lines 241-250 is not the most appropriate for this situation. Please explain why you used this method.*
Give specific suggestions on how to improve the manuscript	*Your introduction needs more detail. I suggest that you improve the description at lines 57- 86 to provide more justification for your study (specifically, you should expand upon the knowledge gap being filled).*
Comment on language and grammar issues	*The English language should be improved to ensure that an international audience can clearly understand your text. Some examples where the language could be improved include lines 23, 77, 121, 128 – the current phrasing makes comprehension difficult. I suggest you have a colleague who is proficient in English and familiar with the subject matter review your manuscript, or contact a professional editing service.*
Organize by importance of the issues, and number your points	*1. Your most important issue* *2. The next most important item* *3. …* *4. The least important points*
Please provide constructive criticism, and avoid personal opinions	*I thank you for providing the raw data, however your supplemental files need more descriptive metadata identifiers to be useful to future readers. Although your results are compelling, the data analysis should be improved in the following ways: AA, BB, CC*
Comment on strengths (as well as weaknesses) of the manuscript	*I commend the authors for their extensive data set, compiled over many years of detailed fieldwork. In addition, the manuscript is clearly written in professional, unambiguous language. If there is a weakness, it is in the statistical analysis (as I have noted above) which should be improved upon before Acceptance.*

New Olenekian austrolimulid from Russia uncovers role of Triassic horseshoe crabs as disaster taxa

Russell D Bicknell [Corresp., 1], **Dmitry E Shcherbakov** [2]

[1] Palaeoscience Research Centre, School of Environmental and Rural Science, University of New England, Armidale, NSW, Australia

[2] Borissiak Paleontological Institute, Russian Academy of Sciences, Moscow, Russia

Corresponding Author: Russell D Bicknell
Email address: rdcbicknell@gmail.com

Horseshoe crabs are archetypal extant marine chelicerates that have an exceptional fossil record extending well into the Palaeozoic. Extreme xiphosurid morphologies arose ~~across~~ their evolutionary history, radiations often reflecting the occupation of freshwater or marginal conditions. This is particularly the case for Austrolimulidae—a xiphosurid family that has recently been subject to thorough taxonomic examination and the description of more species with extreme features. ~~To expand~~ the austrolimulid record, we present new material from the Olenekian-aged Petropavlovka Formation in European Russia and assign this material to *Attenborolimulus superspinosus* gen. et sp. nov. A geometric morphometric analysis of 23 horseshoe crab genera illustrates that the new taxon is distinct from limulid and paleolimulid morphologies, supporting the assignment within Austrolimulidae. In considering Triassic austrolimulids, we suggest that these bizarre forms illustrates that the group functioned as a collection of disaster species after the end-Permian extinction.

New Olenekian austrolimulid from Russia uncovers role of Triassic horseshoe crabs as disaster taxa

Russell D. C. Bicknell[1,*] and Dmitry E. Shcherbakov[2]

[1] Palaeoscience Research Centre, School of Environmental and Rural Science, University of New England, Armidale, New South Wales, 2351, Australia.

[2]Borissiak Paleontological Institute, Russian Academy of Sciences, Profsoyuznaya St 123, Moscow 117647, Russia.

[*]Corresponding author, email: rdcbicknell@gmail.com.

Abstract

Horseshoe crabs are archetypal extant marine chelicerates that have an exceptional fossil record extending well into the Palaeozoic. Extreme xiphosurid morphologies arose across their evolutionary history, radiations often reflecting the occupation of freshwater or marginal conditions. This is particularly the case for Austrolimulidae—a xiphosurid family that has recently been subject to thorough taxonomic examination and the description of more species with extreme features. To expand the austrolimulid record, we present new material from the Olenekian-aged Petropavlovka Formation in European Russia and assign this material to *Attenborolimulus superspinosus* gen. et sp. nov. A geometric morphometric analysis of 23 horseshoe crab genera illustrates that the new taxon is distinct from limulid and paleolimulid morphologies, supporting the assignment within Austrolimulidae. In considering Triassic austrolimulids, we suggest that these bizarre forms illustrates that the group functioned as a collection of disaster species after the end-Permian extinction.

Keywords: Xiphosurida, end-Permian extinction, Triassic recovery, geometric morphometrics, new species, exceptional preservation

Introduction

Examining ecological recovery from the "mother of all extinctions" during the Triassic is important for understanding how biological systems can redevelop after major extinction events (Erwin et al., 2002; Jablonski, 2002; Payne et al., 2004; Twitchett et al., 2004; Dineen et al., 2014). Triassic vertebrate (Hu et al., 2011; Chen & Benton, 2012; Benton et al., 2013; Tintori et al., 2014; Fu et al., 2016), invertebrate (Rodland & Bottjer, 2001; Hu et al., 2011; Chen & Benton, 2012; Hofmann et al., 2013; Fu et al., 2016; Ponomarenko, 2016), and trace (Chen et al., 2012; Crasquin & Forel, 2014; Luo & Chen, 2014; Luo et al., 2019, 2020; Shi et al., 2019; Xing et al., 2021) fossils have been examined to understand recovery of distinct the palaeoecological facets. The arthropod record in particular has shed light on how both marine and terrestrial groups recovered after the end-Permian. Ostracods (Crasquin-Soleau et al., 2007; Forel, 2012; Forel et al., 2013; Crasquin & Forel, 2014; Chu et al., 2015) and insects (Gall & Grauvogel-Stamm, 2005; Shcherbakov, 2008a, b; Hu et al., 2011; Żyła et al., 2013; Ponomarenko, 2016; Zheng et al., 2018; Labandeira & Eble, in press) are commonly examined, with rarer studies of branchiopods (Żyła et al., 2013) and horseshoe crabs (Gall & Grauvogel-Stamm, 2005; Hu et al., 2011; Lerner et al., 2017; Bicknell et al., 2019b). The record of Triassic xiphosurids (so-called horseshoe crabs) has been scrutinised recently; a research trajectory that has uncovered much more information regarding post-Permian taxa (see Błażejowski et al., 2017; Hu et al., 2017; Lerner et al., 2017; Bicknell et al., 2019a, b, 2021a; Bicknell & Pates, 2020; Lamsdell, 2020). Two xiphosurid families are known from the Triassic: Austrolimulidae and Limulidae (Table 1). Of these two, austrolimulids are predominantly marginal marine to freshwater forms with hypertrophied or reduced features. Here, we present new horseshoe crab material from the *Konservat Lagerstätte* within the Petropavlovka Formation, Cis-Urals of Russia to promote the

study of Austrolimulidae and their role in the Triassic recovery of Xiphosurida. This material is also examined using geometric morphometrics to mathematically illustrate the austrolimulid position of these fossils within xiphosurid morphospace. This evidence, coupled with a thorough taxonomic consideration, prompted us to place the Petropavlovka Formation material within a novel genus and species: *Attenborolimulus superspinosus* gen. et sp. nov.

Geological History and Setting

The Permian-Triassic succession of the Cis-Urals is well known for diverse fossil tetrapods and stratigraphic sections that permit detailed study of changes in climate, landscapes, vegetation and biological communities across the Permian–Triassic boundary (Ochev & Shishkin, 1989; Shishkin et al., 1995; Benton et al., 2004; Gomankov, 2005; Shcherbakov, 2008a; Benton & Newell, 2014; Shishkin & Novikov, 2017). The Petropavlovka Formation within this important succession is considered upper Olenekian based on the *Parotosuchus* Otschev & Shishkin (in Kalandadze et al., 1968) tetrapod fauna, the lungfish *Ceratodus multicristatus* (Vorobyeva & Minikh, 1968), miospore assemblages rich in *Densoisporites nejburgii* associated with the lycophyte *Pleuromeia*, and magnetostratigraphy (Figure 1A; Shishkin et al., 1995; Minikh & Minikh, 1997; Tverdokhlebov et al., 2003). During the Olenekian, orogenic movements occurred in the Ural Mountains, while the Peri-Caspian Depression was inundated by the transgression of the Palaeotethys. This resulted in increased rates of siliciclastic deposition in the Cis-Urals (Tverdokhlebov, 1987). In the Cis-Ural Trough and southeastern slope of the Volga-Ural Anteclise, a vast lacustrine-deltaic floodplain was formed. This bordered the northern Peri-Caspian marine basin of the Palaeotethys. The Petropavlovka Formation accumulated in this floodplain. The formation consists of grey and reddish-grey siliciclastics. It is primarily a rhythmic alternation of coarse- and fine-grained

sandstone, clay, siltstone, and fine-grained clayey sandstone, reaching a total thickness of 400–800 m (Shishkin et al., 1995). Conglomerate lenses are also common. Coarser sediment represents alluvial deposits, while finer lithologies constitute shallow water lacustrine deposits. These facies characterise the delta floodplain and delta front complexes that comprise the Petropavlovka Formation (Tverdokhlebov et al., 2003).

The Petropavlovka Formation stratotype section occurs along the Sakmara River and adjacent ravines close to Petropavlovka ~45 km north-east of Orenburg (52º02' N, 55º38' E). Red beds exposed here yield tetrapods, lungfish, clam shrimps, and ostracods (Shishkin et al., 1995). Along one ravine, a one-meter-thick lens of grey fine-grained polymictic siltstone to sandstone was found (locality Petropavlovka III, bed 43; Tverdokhlebov, 1967). The lens contains abundant plant megafossils including sphenophytes and gymnosperms (Dobruskina, 1994). In 2018–2019 numerous diverse insects wings, millipedes, horseshoe crabs, microconchids and a microdrile oligochaete were collected in the lens, along with seed fern pinnules and lycophyte fragments (Hannibal & Shcherbakov, 2019; Shcherbakov et al., 2020, 2021).

Materials & Methods

The studied specimens were collected by the field parties of, and are housed in, the Borissiak Paleontological Institute (PIN), Russian Academy of Sciences, Moscow, Russia. The material was photographed with a Nikon D800 camera mounted with a Nikon AF-S ED Micro Nikkor 60mm f/2.8G lens. Images were z-stacked with Helicon Focus Pro 6.7. Furthermore, a Leica DFC425 camera coupled to Leica M165C stereomicroscope was used. Finally, to examine possible evidence for finer structures, specimens were examined under a TESCAN VEGA scanning electron microscope (SEM) housed at the PIN. Backscattered electron detector was used as the specimens were not coated.

When describing the material, we followed the systematic taxonomy of (Bicknell & Pates, 2020; Bicknell et al., 2021a) and used anatomical terms presented in (Lerner et al., 2017; Bicknell, 2019; Bicknell et al., 2020; Bicknell et al., 2021a).

The geometric morphometric analysis presented here develops on recent applications by Bicknell (2019), Bicknell & Pates (2019), Bicknell et al. (2019b) and Lustri et al. (2021) and assesses where the Petropavlovka Formation material falls morphospace, relative to other xiphosurids. A total of 103 specimens arrayed across 23 genera from Austrolimulidae, Limulidae, and Paleolimulidae (*sensu* Bicknell & Pates, 2020) were considered. Landmarking and semilandmarking was conducted with the Thin-Plate Spline (TPS) suite (http://life.bio.sunysb.edu/morph/index.html). A TPS file was constructed using tpsUtil64 (v.1.7). The TPS file was imported into tpsDig2 (v.2.26), which was used to place four landmarks on the right prosomal section, as well as 50 semi-landmarks along the right prosomal shield border (Figure 2, Supplementary Table 1). Points were digitised as *xy* coordinates. When the right side was poorly preserved, the left side was used, and data mirrored. These points populated the TPS file with landmark data (Supplementary Information 1). The TPS file was imported into R. The 'geomorph' package (Adams et al., 2020) was used to conduct a Procrustes Superimposition and Principal Components Analysis (PCA) of the data (Supplementary Information 2). Only the first two Principal Components (PCs) were considered as they explain 75.6% of the variation in the data (Supplementary Information 3). Bicknell et al. (2019b) demonstrated that the distribution in PC space reflected biological variation. Although preservational mode is varied between specimens (consider Bicknell & Pates, 2020), the variation has little impact on the morphospace as it is dominated by extreme morphologies (see discussion in Lustri et al., 2021). The generic and family assignments presented in Supplemental

Information 3 reflect a combination of taxonomic theses presented in Bicknell & Pates (2020), Lamsdell (2020) and Bicknell et al. (2021a).

The electronic version of this article in Portable Document Format (PDF) will represent a published work according to the International Commission on Zoological Nomenclature (ICZN), and hence the new names contained in the electronic version are effectively published under that Code from the electronic edition alone. This published work and the nomenclatural acts it contains have been registered in ZooBank, the online registration system for the ICZN. The ZooBank LSIDs (Life Science Identifiers) can be resolved and the associated information viewed through any standard web browser by appending the LSID to the prefix http://zoobank.org/. The LSID for this publication is: 5435A6BA-AE34-4698-8872-7A350DB799B1. The online version of this work is archived and available from the following digital repositories: PeerJ, PubMed Central and CLOCKSS.

Systematic Palaeontology

Phylum Euarthropoda Lankester, 1904

Subphylum Chelicerata Heymons, 1901

Order Xiphosurida Latreille, 1802

Suborder Limulina Richter and Richter, 1929

Family Austrolimulidae Riek, 1955

Genus *Attenborolimulus* nov. gen.

Etymology: The generic name is given in honour of Sir David Attenborough and his unparalleled contributions to natural history and conservation. His last name is combined with *Limulus*—the historically oldest xiphosurid genus.

Type species: *Attenborolimulus superspinosus*, new species

Diagnosis. Austrolimulid with anteriorly effaced, ridge-less cardiac lobe, slightly splayed genal spines extending posteriorly to three-fourths of thoracetron length with occipital bands extending to spine terminus, tubercle structures along posterior prosomal and anterior thoracetronic border, medial thoracetronic lobe lacking a ridge, and long, strongly keeled telson

Attenborolimulus superspinosus nov. sp.

Figures 3–8

Etymology: Species name reflects the hypertrophied (*super*-) genal spine (-*spinosus*) morphology.

Holotype: PIN 5640/220 (part and counterpart).

Paratypes: PIN 5640/217, PIN 5640/200 (part and counterpart).

Type locality and horizon. Petropavlovka III near the village of Petropavlovka, Orenburg region, Russia; Petropavlovka Formation, Upper Olenekian, Lower Triassic.

Diagnosis. Same as for genus.

Preservation. Specimens are preserved as partly domed exoskeletons as part and counterpart on yellowish or grey siltstone.

Description. PIN 5640/220 (part and counterpart): An articulated prosoma, thoracetron, and distally incomplete telson (Figures ~~3, 4, 5~~). Specimen is 32.0 mm long as preserved. Prosoma parabolic in outline, 9.8 mm long at midline, and 15.6 mm wide at widest section. Exoskeletal warping along anterior and left lateral prosomal sections. Prosomal rim 0.2 mm wide.

Cephalothoracic doublure 1.6 mm wide, arcuately widened to 2.5 mm medially. Ophthalmic ridges curved towards the lateral prosomal border, ~4.5 mm long. Ridges do not converge anteriorly. Lateral compound eyes narrow reniform, ~ 2.9 mm long, ~ 0.7 mm wide, inner orbita 4.1 mm from midline. Cardiac lobe 7.5 mm long, 4.1 mm wide posteriorly, tapering to its mid-length, about 2.0 mm wide in anterior half, tapered to 1.4 mm near apex, effaced anteriorly. Break in left genal spine within first quarter of thoracetron. Posterior-most left genal section 8.4 mm from midline. Angle between left genal spine and left thoracetron side 77.2°. Right genal spine complete, terminates three fourths along thoracetron. Genal spine terminus 7.8 mm from midline, 6.9 mm from level of prosomal-thoracetronic hinge. Angle between right genal spine and right thoracetron side 38.5°. Pronounced occipital bands extend from ophthalmic ridges to genal spine ends. Prosomal-thoracetronic hinge pronounced, 7.6 mm wide, and 0.6 mm long. Posterior prosomal border with shallow central notch 2.1 mm wide. Distal sections of prosomal appendages noted lateral to compound eyes (Figure 3B).

Thoracetron trapezoidal, completely preserved in counterpart (Figures 3, 5C), 8.1 mm long at midline, 9.4 mm wide anteriorly, tapering to 4.7 mm posteriorly. Tubercle structures along anterior thoracetron border noted under SEM (Figure 5D). Thoracetronic flange present. Rounded anterolateral lobes apparently present. Setose margins of branchial appendages (opercula) visible anteriorly on left side in counterpart. Medial thoracetronic lobe weakly defined, 7.3 mm long, 3.0 mm anteriorly, tapering to 1.2 mm posteriorly. Lobe lacking medial thoracetronic ridge. Left pleural lobe has 0.3 mm wide rim. Left lobe 8.0 mm long, 2.6 mm wide, tapering posteriorly to short, round terminal spine. Right lobe damaged in part. Measurements taken from counterpart. Right lobe 8.2 mm long, 2.5 mm wide, tapering posteriorly to short, rounded terminal spine. Minute fixed spines and movable spine notches observed under SEM on

left side of thoracetron (Fig. 5C). Telson 14.1 mm long as preserved, with well-developed keel. Telson terminates at rock edge, has a kink at a third of the spine length.

PIN 5640/200 (part and counterpart): Isolated prosoma preserved more completely in part (Figures 5B, 6). Prosoma parabolic in outline, 15.1 mm long at midline, and 26.8 mm wide at widest section. Exoskeletal warping along anterior and right lateral prosomal sections. Prosomal rim 0.6 mm wide. Cephalothoracic doublure 2.1 mm wide, arcuately widened backwards up to 4.1 mm medially. Right ophthalmic ridge noted in counterpart (Figure 6C, D). Ridge curved towards the lateral prosomal border, 9.1 mm long. Lateral compound eyes narrow reniform, ~ 3.7 mm long, ~ 0.8 mm wide, right inner orbita 7.5 mm from midline. Cardiac lobe present, 7.5 mm long, 6.8 mm wide posteriorly, tapering (more so posteriorly and anteriorly) to 1.8 mm, effaced anteriorly. Left genal spine broken distally. Most distal left genal section 13.9 mm from midline. Right genal spine complete, lateral margin slightly convex. Genal spine terminus 14.1 mm from midline, 13.6 mm from level of prosomal-thoracetronic hinge. Pronounced occipital bands extend from ophthalmic ridges to genal spine ends, better preserved along right genal spine. Ridge delimiting occipital band with tubercles along posterior prosomal border and near base of genal spines. Posterior prosomal border with arcuate central notch 4.3 mm wide. Clam shrimps (round structures) noted.

PIN 5640/217: Central and left side of prosoma (Figure 7), 15.4 mm long at midline, and 17.1 mm wide at widest section. Prosomal rim 0.3 mm wide. Partial left ophthalmic ridge noted. Cardiac lobe 9.0 mm long, 7.0 mm wide posteriorly, tapering slightly anteriorly to 2.5 mm, effaced anteriorly. Anterior most section of left genal spine noted. Two round structures on left side of prosoma, tentaculitoid tubeworms (Shcherbakov et al., 2021).

Remarks: The horseshoe crab material documented herein displays hypertrophied genal spines, a feature common in Belinurina and Austrolimulidae. The examined material lacks complete expression of thoracetronic tergites and a rounded thoracetron common to Belinurina. Furthermore, as Belinurina went extinct by the end-Permian, the Petropavlovka Formation specimens belong in Austrolimulidae. Bicknell et al. (2020) outlined two major groupings of austrolimulids: those with reduced thoracetronic sections relative to the prosoma and those with genal spines that extend up to the thoracetron terminus. Prosomal and thoracetronic sections of the Petropavlovka Formation specimens are comparable, excluding this material from the first group Bicknell et al. (2020) outlined. This differentiates the material considered here from, *Batracholimulus fuchsbergensis* (Hauschke & Wilde, 1987), *Boeotiaspis longispinus* (Schram, 1979), *Dubbolimulus peetae* Pickett, 1984, *Panduralimulus babcocki* Allen & Feldmann, 2005, and *Shpineviolimulus jakovlevi* (Glushenko & Ivanov, 1961). Comparisons to *Austrolimulus fletcheri* Riek, 1955, *Franconiolimulus pochankei* Bicknell, Hecker & Heyng, 2021, *Psammolimulus gottingensis* Lange, 1923, *Tasmaniolimulus patersoni* Bicknell, 2019, and *Vaderlimulus tricki* Lerner, Lucas & Lockley, 2017 are therefore needed—austrolimulids with hypertrophied genal spines. *Austrolimulus fletcheri* and *V. tricki* both have hypertrophied genal spines with extensive splay, not observed in the Petropavlovka Formation material (Riek, 1955, 1968; Lerner et al., 2017). *Franconiolimulus pochankei*, the youngest austrolimulid, has a cardiac ridge, distally effaced occipital bands, and a thoracetronic free lobe, none of which are observed in the Petropavlovka Formation material. *Tasmaniolimulus patersoni* has pronounced thoracetronic free lobes, as well as keeled cardiac and medial thoracetronic lobes (Ewington et al., 1989; Bicknell, 2019). These are not observed in the Petropavlovka Formation material, excluding the new fossils from this Lopingian genus. *Psammolimulus gottingensis* is the most

morphologically similar to the new material. Indeed, the genal spine morphology and pronounced occipital bands suggest a strong alignment with *P. gottingensis* (Meischner, 1962). However, *P. gottingensis* has hypertrophied terminal thoracetronic spines and pronounced free lobes. Neither of these features are observed in the specimens examined here. B Based on this comparison, we assert that the Petropavlovka Formation material is morphologically distinct from other austrolimulids enough to be separated at the generic level, as *Attenborolimulus superspinosus* gen. et sp. nov. This taxonomic assessment is supported by geometric morphometric results (see Results).

One point to consider is *Limulitella* Størmer, 1952 as an austrolimulid genus. Lamsdell (2020) recently used tree topology to propose that *Limulitella* fell into Austrolimulidae, suggesting that the family consisted of limuloids with "apodemal pits present on thoracetron; thoracetron lacking tergopleural fixed spines; posteriormost thoracetron tergopleurae swept back and elongated to form 'swallowtail'; axis of thoracetron bearing dorsal keel" (Lamsdell, 2020, p. 20). Examining *L. bronnii* (Schimper, 1853), for example, specimens have evidence of fixed spines, rendering the placement of *Limulitella* within Austrolimulidae tenuous. We have therefore not compared *Attenborolimulus superspinosus* to *Limulitella* species, as it seems more likely that the group are limulids (*sensu* Bicknell & Pates, 2020; Bicknell et al., 2021a).

Results

PCA plot shows that PC1 (48.3% shape variation) describes how laterally the most distal genal spine point extends from the sagittal line (Figure 9). PC2 (27.3% shape variation) describes how posteriorly the genal spine projects, relative to the prosomal midline and posterior border. Paleolimulids and limulids are both located in PC1 space <0.05, reflecting the lack of genal splay observed in the groups. Specimens within Austrolimulidae cover PC1 space from 0–0.3

reflecting the variation in genal spine splay observed in the family. The holotype of *Attenborolimulus superspinosus* gen. et sp. nov. is located in a positive PC1 space (PC1=0.099) and a neutral PC2 space (PC2 = 0.002) (Figures 9, 10). It falls outside the morphospace occupied by Limulidae and Paleolimulidae (Figure 9) and ~~outside~~ distribution of other austrolimulid genera (Figure 10).

Discussion

The meter-thick lens that yielded *Attenborolimulus* gen. nov. is a rare occurrence of grey lithologies among the red beds of the Petropavlovka Formation. These red beds yield the lungfish *Ceratodus*, temnospondyl amphibians, and procolophonid and erythrosuchid reptiles (Shishkin et al., 1995; Novikov, 2018). The grey lens contains a different set of fossils: abundant, but fragmentary vascular plants, numerous insects (mainly isolated wings of various roaches, beetles, hemipterans, and rare dragonflies, grylloblattids and orthopterans), microconchids, rare millipedes, and a microdrile oligochaete (Hannibal & Shcherbakov, 2019; Shcherbakov et al., 2020, 2021). Clam shrimps and ostracods recorded in the grey bed occur in surrounding red beds as well. Notably, plant and animal fossils are not restricted to certain bedding planes but are randomly distributed in the rock, thus preserving some three-dimensionality. Such a sediment probably accumulated in an ephemeral pond during a flood event. The millipedes, most plants and nearly all insects, the remains of which were washed into the water body from the land, are allochthonous fossils. The horsetails *Equisetites* and *Neocalamites* likely grew as helophytes protruding out of the water, because some fragments of their stems are encrusted with microconchid shells. The aquatic ecosystem is represented by (sub)autochthonous fossils of ceratodontid lungfishes, numerous schizophoroid beetle adults, clam shrimps, ostracods, horseshoe crabs, microdriles, and microconchids. The unique microdrile specimen is the earliest

fossil record of oligochaete annelids. This small worm is similar to modern tubificids, and its relatively well developed body wall musculature suggests that sediment burrowing was originally another way to escape desiccation on the bottom of seasonally drying ponds (Shcherbakov et al., 2020). Minute microconchids that encrusted plant stems, horseshoe crab exuvia and other available firm substrates represent the major suspension feeders in the Petropavlovka ecosystem. These extinct lophophorates were genuine disaster taxa—eurytopic stress-tolerators that flourished in the aftermath of the end-Permian extinction in both marine and continental basins all over the world (Shcherbakov et al., 2021). Dense accumulations of primarily pyrite dodecahedra are common on attached microconchid tubes, stem veins and rootlets. A high carbon/sulphur ratio might be expected for the appearance of abundant pyrite clusters in a freshwater basin (Hethke et al., 2013). Also, the decomposition of organic matter by sulphate-reducing bacteria favoured increased acidity and would lead to the precipitation of early diagenetic pyrite (Fürsich & Pan, 2016). This sedimentological feature might be indicative of abundant decaying plant and animal remains consumed by bacteria at the lake bottom, but not for the redox state of the water column itself. However, a lacustrine palaeocoenosis, including ceratodontid lungfishes capable of aestivation in their burrows, horseshoe crabs, microdriles and abundant microconchids, points to a meromictic eutrophic lake.

Vacant ecological space is a key factor in allowing evolutionary innovation to develop (Erwin, 2008). Triassic austrolimulids were able to capitalise on vacant marginal to freshwater environs, thus exploiting an unprecedented array of niches. The high xiphosurid Triassic diversity and disparity, followed by a constrained morphology from the Jurassic through to today suggest after the end-Permian xiphosurids functioned as disaster taxa: groups with a long evolutionary history that invade and exploit vacant ecospace during a post-extinction, survival

stage (Rodland & Bottjer, 2001). The presence of exclusively limulid species after the Early Triassic records the extinction of these opportunistic forms (Bicknell et al., 2021b) and the transition to a morphology that was conserved through into modern ecosystems (Bicknell & Pates, 2020). The hypertrophied genal spines observed in austrolimulids also illustrate evolutionary convergence with the belinurids *Euproops* Meek, 1867 and *Belinurus* Pictet, 1846. The prevalence of this trait in two distinct xiphosurid families demonstrates how colonisation of marginal conditions placed similar evolutionary constraints on the xiphosurid *Bauplan*, resulting in comparable morphologies.

Declarations

Ethics Approval and Consent to Participate

Not applicable.

Consent for Publication

Not applicable.

Authors' Contributions

RDCB conceived the project, developed the methods and wrote the first draft. DES collected and identified the fossils, and took photographs and collated other images and presented the geological and palaeontological information. Both authors constructed figures. Both authors reviewed and edited the text.

Acknowledgments

This research was supported by funding from a University of New England Postdoctoral Research Fellowship (to R.D.C.B.). The field work was supported by the Russian Foundation

317 grant 21-14-00284 (to D.E.S.). We are deeply grateful to Anastasia Felker, Elena Lukashevich,
318 Olesya Strelnikova, Maria Tarasenkova, Alexey Bashkuev and Dmitry Vasilenko who
319 participated in fossil hunting, and especially to Eugeny Karasev who found the future holotype,
320 to Sergey Bagirov for the excellent photographs, to Roman Rakitov for his help in obtaining
321 perfect SEM images, and to Andrey Sennikov (all PIN) and Valentin Tverdokhlebov (Saratov
322 State University) for information on the fossil locality.

323 **References**

324 **Adams DC, Collyer ML, Kaliontzopoulou A**. **2020**. Geomorph: Software for geometric
325 morphometric analyses. R package version 3.2.1. *https://cranr-projectorg/package=geomorph*:
326 **Allen JG, Feldmann RM**. **2005**. *Panduralimulus babcocki* n. gen. and sp., a new Limulacean
327 horseshoe crab from the Permian of Texas. *Journal of Paleontology* **79 (3)**: 594–600.
328 **Benton MJ, Newell AJ**. **2014**. Impacts of global warming on Permo-Triassic terrestrial
329 ecosystems. *Gondwana Research* **25 (4)**: 1308–1337.
330 **Benton MJ, Tverdokhlebov VP, Surkov MV**. **2004**. Ecosystem remodelling among vertebrates
331 at the Permian–Triassic boundary in Russia. *Nature* **432 (7013)**: 97–100.
332 **Benton MJ, Zhang Q, Hu S, Chen Z-Q, Wen W, Liu J, Huang J, Zhou C, Xie T, Tong J**.
333 **2013**. Exceptional vertebrate biotas from the Triassic of China, and the expansion of marine
334 ecosystems after the Permo-Triassic mass extinction. *Earth-Science Reviews* **125**: 199–243.
335 **Bicknell RDC**. **2019**. Xiphosurid from the Upper Permian of Tasmania confirms Palaeozoic
336 origin of Austrolimulidae. *Palaeontologia Electronica* **22 (3)**: 1–13.
337 **Bicknell RDC, Błażejowski B, Wings O, Hitij T, Botton ML**. **2021a**. Critical re-evaluation of
338 Limulidae reveals limited *Limulus* diversity. *Papers in Palaeontology*: 1–32.

Bicknell RDC, Brougham T, Charbonnier S, Sautereau F, Hitij T, Campione NE. **2019a**. On the appendicular anatomy of the xiphosurid *Tachypleus syriacus* and the evolution of fossil horseshoe crab appendages. *The Science of Nature* **106 (7)**: 38.

Bicknell RDC, Hecker A, Heyng AM. **2021b**. New horseshoe crab fossil from Germany demonstrates post-Triassic extinction of Austrolimulidae. *Geological Magazine*: 1–11.

Bicknell RDC, Naugolnykh SV, Brougham T. **2020**. A reappraisal of Paleozoic horseshoe crabs from Russia and Ukraine. *The Science of Nature* **107**: 46.

Bicknell RDC, Pates S. **2019**. Xiphosurid from the Tournaisian (Carboniferous) of Scotland confirms deep origin of Limuloidea. *Scientific Reports* **9 (1)**: 17102.

Bicknell RDC, Pates S. **2020**. Pictorial atlas of fossil and extant horseshoe crabs, with focus on Xiphosurida. *Frontiers in Earth Science* **8 (98)**: 60.

Bicknell RDC, Žalohar J, Miklavc P, Celarc B, Križnar M, Hitij T. **2019b**. A new limulid genus from the Strelovec Formation (Middle Triassic, Anisian) of northern Slovenia. *Geological Magazine* **156 (12)**: 2017–2030.

Błażejowski B, Niedźwiedzki G, Boukhalfa K, Soussi M. **2017**. *Limulitella tejraensis*, a new species of limulid (Chelicerata, Xiphosura) from the Middle Triassic of southern Tunisia (Saharan Platform). *Journal of Paleontology* **91 (5)**: 960–967.

Bleicher M-G. **1897**. Sur la découverte d'une nouvelle espèce de limule dans les marnes irisées de Lorraine. *Bulletin de la Societe des Sciences de Nancy* **2**: 116–126.

Braun KFW. **1860**. Die Thiere in den Pflanzenschiefern der Gegend von Bayreuth. *Jahresbericht von der König Kreis-Landwirtschafts- und Gewerbschule zu Bayreuth für das Schuljahr 1859/60*:

Chen Z-Q, Benton MJ. **2012**. The timing and pattern of biotic recovery following the end-Permian mass extinction. *Nature Geoscience* **5 (6)**: 375–383.

Chen Z-Q, Fraiser ML, Bolton C. **2012**. Early Triassic trace fossils from Gondwana Interior Sea: implication for ecosystem recovery following the end-Permian mass extinction in south high-latitude region. *Gondwana Research* **22 (1)**: 238–255.

Chu D, Tong J, Song H, Benton MJ, Song H, Yu J, Qiu X, Huang Y, Tian L. **2015**. Lilliput effect in freshwater ostracods during the Permian–Triassic extinction. *Palaeogeography, Palaeoclimatology, Palaeoecology* **435**: 38–52.

Crasquin-Soleau S, Galfetti T, Bucher H, Kershaw S, Feng Q. **2007**. Ostracod recovery in the aftermath of the Permian-Triassic crisis: Palaeozoic-Mesozoic turnover. *Hydrobiologia* **585**: 13–27.

Crasquin S, Forel M-B. **2014**. Ostracods (Crustacea) through Permian–Triassic events. *Earth-Science Reviews* **137**: 52–64.

Dineen AA, Fraiser ML, Sheehan PM. **2014**. Quantifying functional diversity in pre-and post-extinction paleocommunities: a test of ecological restructuring after the end-Permian mass extinction. *Earth-Science Reviews* **136**: 339–349.

Dobruskina IA. **1994**. *Triassic Floras of Eurasia*. Wein, New York: Springer.

Erwin DH. **2008**. Extinction as the loss of evolutionary history. *Proceedings of the National Academy of Sciences* **105 (Supplement 1)**: 11520–11527.

Erwin DH, Bowring SA, Yugan J. **2002**. End-Permian mass extinctions: a review. In: Koeberl C, and MacLeod KC, eds. *Catastrophic Events and Mass Extinctions: Impacts and Beyond Special Paper 356*. Boulder: Geological Society of America, 363–384.

Ewington DL, Clarke MJ, Banks MR. **1989**. A Late Permian fossil horseshoe crab (*Paleolimulus*: Xiphosura) from Poatina, Great Western Tiers, Tasmania. *Papers and Proceedings of the Royal Society of Tasmania* **123**: 127–131.

Forel M-B. **2012**. Ostracods (Crustacea) associated with microbialites across the Permian-Triassic boundary in Dajiang (Guizhou Province, south China). *European Journal of Taxonomy* **19**: 1–34.

Forel M-B, Crasquin S, Hips K, Kershaw S, Collin P-Y, Haas J. **2013**. Biodiversity evolution through the Permian—Triassic boundary event: Ostracods from the Bükk Mountains, Hungary. *Acta Palaeontologica Polonica* **58 (1)**: 195–219.

Fu W, Jiang D-y, Montañez IP, Meyers SR, Motani R, Tintori A. **2016**. Eccentricity and obliquity paced carbon cycling in the Early Triassic and implications for post-extinction ecosystem recovery. *Scientific Reports* **6 (1)**: 1–7.

Fürsich FT, Pan Y. **2016**. Diagenesis of bivalves from Jurassic and Lower Cretaceous lacustrine deposits of northeastern China. *Geological Magazine* **153 (1)**: 17–37.

Gall J-C, Grauvogel-Stamm L. **2005**. The early Middle Triassic 'Grès à Voltzia' Formation of eastern France: a model of environmental refugium. *Comptes Rendus Palevol* **4 (6-7)**: 637–652.

Glushenko NV, Ivanov VK. **1961**. *Paleolimulus* from the Lower Permian of the Donetz Basin. *Paleontologiceskij Žurnal* **1961 (2)**: 128–130.

Gomankov AV. **2005**. Floral changes across the Permian-Triassic boundary. *Stratigraphy and Geological Correlation* **13 (2)**: 74–83.

Hannibal JT, Shcherbakov DE. **2019**. New tomiulid millepedes from the Triassic of European Russia and a re-evaluation of the type material of *Tomiulus angulatus* from the Permian of

Siberia. In: Dányi L, Korsós Z, and Lazányi E, eds. 18th International Congress of Myriapodology: Hungarian Natural History Museum, Hungarian Biological Society. p 25–31.

Hauschke N, Wilde V. **1987**. *Paleolimulus fuchsbergensis* n. sp. (Xiphosura, Merostomata) aus der oberen Trias von Nordwestdeutschland, mit einer Übersicht zur Systematik und Verbreitung rezenter Limuliden. *Paläontologische Zeitschrift* **61 (1/2)**: 87–108.

Hethke M, Fürsich FT, Jiang B, Klaus R. **2013**. Oxygen deficiency in Lake Sihetun; formation of the Lower Cretaceous Liaoning Fossillagerstätte (China). *Journal of the Geological Society* **170 (5)**: 817–831.

Heymons R. **1901**. Die Entwicklungsgeschichte der Scolopender. *Zoologica* **13**: 1–244.

Hofmann R, Hautmann M, Wasmer M, Bucher H. **2013**. Palaeoecology of the Spathian Virgin Formation (Utah, USA) and its implications for the Early Triassic recovery. *Acta Palaeontologica Polonica* **58 (1)**: 149–173.

Hu S-x, Zhang Q-y, Chen Z-Q, Zhou C-y, Lü T, Xie T, Wen W, Huang J-y, Benton MJ. **2011**. The Luoping biota: exceptional preservation, and new evidence on the Triassic recovery from end-Permian mass extinction. *Proceedings of the Royal Society B: Biological Sciences* **278 (1716)**: 2274–2282.

Hu S, Zhang Q, Feldmann RM, Benton MJ, Schweitzer CE, Huang J, Wen W, Zhou C, Xie T, Lü T, Hong S. **2017**. Exceptional appendage and soft-tissue preservation in a Middle Triassic horseshoe crab from SW China. *Scientific Reports* **7 (1)**: 14112.

Jablonski D. **2002**. Survival without recovery after mass extinctions. *Proceedings of the National Academy of Sciences* **99 (12)**: 8139–8144.

Kalandadze NN, Ochev VG, Tatarinov LP, Chudinov PK, Shishkin MA. **1968**. Katalog permskikh i triasovykh tetrapod SSSR. *Doklady Akademii Nauk SSSR* **179**: 72–91.

Labandeira CC, Eble GJ. **in press**. The fossil record of insect diversity and disparity. In: Anderson J, Thackeray F, Wyk BV, and Wit MD, eds. *Gondwana alive: biodiversity and the evolving biosphere*: Witwatersrand University Press.

Lamsdell JC. **2020**. The phylogeny and systematics of Xiphosura. *PeerJ* **8**: e10431.

Lange W. **1923**. Über neue Fossilfunde aus der Trias von Göttingen. *Zeitschrift der deutschen geologischen Gesellschaft* **74**: 162–168.

Lankester ER. **1904**. The structure and classification of Arthropoda. *Quarterly Journal of Microscopial Science* **47**: 523–582.

Latreille PA. **1802**. *Histoire naturelle, générale et particulière, des crustacés et des insectes*. Paris: Dufart.

Lerner AJ, Lucas SG, Lockley M. **2017**. First fossil horseshoe crab (Xiphosurida) from the Triassic of North America. *Neues Jahrbuch für Geologie und Paläontologie-Abhandlungen* **286 (3)**: 289–302.

Luo M, Chen ZQ. **2014**. New arthropod traces from the Lower Triassic Kockatea Shale formation, northern Perth Basin, Western Australia: ichnology, taphonomy and palaeoecology. *Geological Journal* **49 (2)**: 163–176.

Luo M, Shi GR, Buatois LA, Chen Z-Q. **2020**. Trace fossils as proxy for biotic recovery after the end-Permian mass extinction: A critical review. *Earth-Science Reviews* **203**: 103059.

Luo M, Shi GR, Hu S, Benton MJ, Chen Z-Q, Huang J, Zhang Q, Zhou C, Wen W. **2019**. Early Middle Triassic trace fossils from the Luoping Biota, southwestern China: Evidence of recovery from mass extinction. *Palaeogeography, Palaeoclimatology, Palaeoecology* **515**: 6–22.

Lustri L, Laibl L, Bicknell RDC. **2021**. A revision of *Prolimulus woodwardi* Fritsch, 1899 with comparison to other paedomorphic belinurids. *PeerJ* **9**: e10980.

Meek FB. **1867**. Notes on a new genus of fossil Crustacea. *Geological Magazine, Decade* **4**: 320–321.

Meischner K-D. **1962**. Neue Funde von *Psammolimulus gottingensis* (Merostomata, Xiphosura) aus dem Mittleren Buntsandstein von Göttingen. *Paläontologische Zeitschrift* **36 (1)**: 185–193.

Minikh MG, Minikh AV. **1997**. Ichthyofaunal correlation of the Triassic deposits from the northern Cis-Caspian and southern Cis-Urals regions. *Geodiversitas* **19 (2)**: 279–292.

Novikov IV. **2018**. Early Triassic amphibians of Eastern Europe: Evolution of dominant groups and traits of changing communities (in Russian). *Transactions of Paleontological Institute, Russian Academy of Sciences* **296**: 1–358.

Ochev WG, Shishkin MA. **1989**. On the principles of global correlation at the continental Triassic on the tetrapods. *Acta Palaeontologica Polonica* **34 (2)**: 149–173.

Payne JL, Lehrmann DJ, Wei J, Orchard MJ, Schrag DP, Knoll AH. **2004**. Large perturbations of the carbon cycle during recovery from the end-Permian extinction. *Science* **305 (5683)**: 506–509.

Pickett JW. **1984**. A new freshwater limuloid from the middle Triassic of New South Wales. *Palaeontology* **27 (3)**: 609–621.

Pictet F-J. **1846**. *Traité Élémentaire De Paléontologie Ou Histoire Naturelle Des Animaux Fossiles*: Baillière.

Ponomarenko AG. **1985**. King crabs and eurypterids from the Permian and Mesozoic of the USSR. *Paleontological Journal* **19**: 100–104.

Ponomarenko AG. **2016**. Insects during the time around the Permian—Triassic crisis. *Paleontological Journal* **50 (2)**: 174–186.

Richter R, Richter E. **1929**. *Weinbergina opitzi* n. g, n. sp., ein Schwertträger (Merost., Xiphos.) aus dem Devon (Rheinland). *Senckenbergiana* **11**: 193–209.

Riek EF. **1955**. A new xiphosuran from the Triassic sediments at Brookvale, New South Wales. *Records of the Australian Museum* **23 (5)**: 281–282.

Riek EF. **1968**. Re-examination of two arthropod species from the Triassic of Brookvale, New South Wales. *Records of the Australian Museum* **27 (17)**: 313–321.

Rodland DL, Bottjer DJ. **2001**. Biotic recovery from the end-Permian mass extinction: behavior of the inarticulate brachiopod *Lingula* as a disaster taxon. *Palaios* **16 (1)**: 95–101.

Romero PA, Vía Boada L. **1977**. Tarracolimulus rieke nov. gen., nov. sp., nuevo Limulido del Triasico de Montral-Alcover (Tarragona). *Cuadernos Geologia Ibérica* **4**: 239–246.

Schimper W-P. **1853**. Palaeontologica alsatica: ou fragments paléontologiques des différents terrains stratifiés qui se rencontrent en Alsace. *Mémoires de la Société du Muséum d'Histoire Naturelle de Strasbourg* **4**: 1–10.

Schram FR. **1979**. Limulines of the Mississippian Bear Gulch Limestone of Central Montana, USA. *Transactions of the San Diego Society of Natural History* **19 (6)**: 67–74.

Shcherbakov DE. **2008a**. Insect recovery after the Permian/Triassic crisis. *Alavesia* **2**: 125–131.

Shcherbakov DE. **2008b**. On Permian and Triassic insect faunas in relation to biogeography and the Permian-Triassic crisis. *Paleontological Journal* **42 (1)**: 15–31.

Shcherbakov DE, Timm T, Tzetlin AB, Vinn O, Zhuravlev AY. **2020**. A probable oligochaete from an Early Triassic Lagerstätte of the southern Cis-Urals and its evolutionary implications. *Acta Palaeontologica Polonica* **65 (2)**: 219–233.

Shcherbakov DE, Vinn O, Zhuravlev AY. **2021**. Disaster microconchids from the uppermost Permian and Lower Triassic lacustrine strata of the Cis-Urals and the Tunguska and Kuznetsk basins (Russia). *Geological Magazine*: 1–23.

Shi G, Woods AD, Yu M-Y, Li X-W, Wei H-Y, Qiao D. **2019**. Lower Triassic limulid trackways (*Kouphichnium*) from the southwestern margin of the Yangtze carbonate platform: paleoenvironmental and paleoecological implications. *Palaios* **34 (4)**: 229–243.

Shishkin MA, Novikov IV. **2017**. Early stages of recovery of the East European tetrapod fauna after the end-Permian crisis. *Paleontological Journal* **51 (6)**: 612–622.

Shishkin MA, Ochev VG, Tverdokhlebov VP, Vergay IF, Gomankov AV, Kalandadze NN, Leonova EM, Lopato AY, Makarova IS, Minikh MG, Molostovskiy EM, Novikov IV, Sennikov AG. **1995**. *Biostratigrafiya kontinental'nogo triasa yuzhnogo Predural'ya (Biostratigraphy of the Continental Triassic in the Southern Cis-Urals) (in Russian)*. Moscow: Nauka.

Størmer L. **1952**. Phylogeny and taxonomy of fossil horseshoe crabs. *Journal of Paleontology* **26 (4)**: 630–640.

Tintori A, Hitij T, Jiang D, Lombardo C, Sun Z. **2014**. Triassic actinopterygian fishes: the recovery after the end-Permian crisis. *Integrative Zoology* **9 (4)**: 394–411.

Tverdokhlebov VP. **1967**. Petropavlovka, Berezovy. In: Morozov NS, ed. *Putevoditel' ekskursii po verhnepermskim i triasovym kontinental'nym obrazovaniyam yugo-vostoka Russkoy platformy i Priural'ya (Guidebook of the Excursion on Upper Permian and Triassic Continental Formations of the South-East of the Russian Platform and the Cis-Urals) (In Russian)*. Saratov: Saratovskiy Gosudarstvennyy Universitet imeni N. G. Chernyshevskogo, Orenburgskoe Geologicheskoe Upravlenie, 109–148.

Tverdokhlebov VP. **1987**. Triasovye ozera Yuzhnogo Priural'ya (Triassic lakes of the southern Cis-Urals. In: Martinson GG, and Neustrueva IY, eds. *Istoriya ozer pozdnego paleozoya i rannego mezozoya (Late Palaeozoic and Early Mesozoic Lake History) (In Russian)* Leningrad: Nauka, 235–242.

Tverdokhlebov VP, Tverdokhlebova GI, Surkov MV, Benton MJ. **2003**. Tetrapod localities from the Triassic of the SE of European Russia. *Earth-Science Reviews* **60 (1-2)**: 1–66.

Twitchett RJ, Krystyn L, Baud A, Wheeley JR, Richoz S. **2004**. Rapid marine recovery after the end-Permian mass-extinction event in the absence of marine anoxia. *Geology* **32 (9)**: 805–808.

Vía Boada L. **1987**. Artropodos fosiles Triasicos de Alcover-Montral. II. Limulidos. *Cuadernos Geología Ibérica* **11**: 281–294.

Vía L, De Villalta JF. **1966**. *Hetrolimulus gadeai*, nov. gen., nov. sp., représentant d'une nouvelle famille de Limulacés dans le Trias d'Espagne. *Comtes Rendues Sommaire Séances Societé Géologique France* **8**: 57–59.

von Fritsch KWG. **1906**. Beitrag zur Kenntnis der Tierwelt der deutschen Trias. *Abhandlungen der naturforschender Gesellschaft Halle* **24**: 220–285.

Vorobyeva EI, Minikh MG. **1968**. Experimental application of biometry to the study of ceratodontid dental plates (In Russian). *Paleontological Journal* **2**: 76–87.

Xing Z-F, Lin J, Fu Y-X, Zheng W, Liu Y-L, Qi Y-A. **2021**. Trace fossils from the Lower Triassic of North China—a potential signature of the gradual recovery of a terrestrial ecosystem. *Palaeoworld* **30**: 95–105.

Zhang QY, Hu SX, Zhou CY, Lü T, Bai JK. **2009**. First occurrence of horseshoe crab (Arthropoda) fossils from China. *Progress in Natural Science* **19**: 1090–1093.

Zheng D, Chang S-C, Wang H, Fang Y, Wang J, Feng C, Xie G, Jarzembowski EA, Zhang H, Wang B. **2018**. Middle-Late Triassic insect radiation revealed by diverse fossils and isotopic ages from China. *Science Advances* **4 (9)**: eaat1380.

Żyła D, Wegierek P, Owocki K, Niedźwiedzki G. **2013**. Insects and crustaceans from the latest Early–early Middle Triassic of Poland. *Palaeogeography, Palaeoclimatology, Palaeoecology* **371**: 136–144.

Figure Captions

Figure 1: Geographical and geological information for the studied fossil site. (A) Map showing locality of Petropavlovka III (red star). (B) Stratigraphic log of Petropavlovka II–IV sections showing location of horseshoe crab-bearing lens (modified from Tverdokhlebov, 1967).

Figure 2: Depiction of geometric morphometric data gathered here: four landmarks and one semilandmark outline. Consider Supplementary Table 1 for description of landmarks.

Figure 3: Holotype of *Attenborolimulus superspinosus* gen. et sp. nov. PIN 5640/220, counterpart.

Figure 4: Holotype of *Attenborolimulus superspinosus* gen. et sp. nov., PIN 5640/220, part. (A, B): Photograph and interpretative drawing. Image credit: Dmitry Shcherbakov. Abbreviations: Car: cardiac lobe; Fla: thoracetronic flange; Med: medial thoracetronic lobe; Oph: ophthalmic ridge; Pa: prosomal appendage; Pro: prosoma; Thr: thoracetron; Tel: telson.

Figure 5: SEM images of the *Attenborolimulus superspinosus* gen. et sp. nov. (A, C, D): Holotype, PIN 5640/220, counterpart. (A) Entire specimen. (C) Close up of box in (A), showing small moveable spine notches and fixed spines (white arrows). (D): Close up of box in (A), showing tubercles along prosomal thoracetronic border (white arrows). (B): Paratype, PIN 5640/200, part. Image credit: Dmitry Shcherbakov.

Figure 6: Paratype PIN 5640/200 of *Attenborolimulus superspinosus* gen. et sp. nov. showing key prosomal features. (A, B): Part, photograph and interpretative drawing. (C, D): Counterpart, photograph and interpretative drawing. Image credit: Dmitry Shcherbakov. Abbreviations: Car: cardiac lobe.

569 **Figure 7:** Paratype PIN 5640/217 of *Attenborolimulus superspinosus* gen. et sp. nov. (A, B):
570 Photograph and interpretative drawing. Image credit: Sergey Bagirov.

571 **Figure 8.** Reconstruction of *Attenborolimulus superspinosus* gen. et sp. nov. Reconstruction
572 credited to Katrina Kenny.

573 **Figure 9.** Three examined xiphosurids families in PC space. Austrolimulids occupy most
574 positive PC1 space while limulids and paleolimulids are mostly constrained to negative PC1
575 space. *Attenborolimulus superspinosus* gen. et sp. nov. falls within the convex hull occupied by
576 Austrolimulidae. Note that the austrolimulid morphospace excludes *Limulitella* specimens, as the
577 position of this genus in Austrolimulidae is considered dubious.

578 **Figure 10.** PC plot showing morphospace occupied by xiphosurid genera. Where more than one
579 specimen was digitised, genera are bound by convex hulls. *Attenborolimulus superspinosus* gen.
580 et sp. nov. is not bound by any convex hull, excluding the specimen from other genera.

581 **Supplementary Information 1**: TPS file of analysed specimens.
582 **Supplementary Information 2**: CSV file used for semilandmark sliding.
583 **Supplementary Information 3**: CSV file of PCA results. Includes family, generic and temporal
584 data.

Taxon	Family	Formation, locality	Age	Depositional environment
Austrolimulus fletcheri Riek, 1955	Austrolimulidae	Beacon Hill Shale, New South Wales, Australia	Middle Triassic (Ladinian)	Marginal marine to freshwater
Attenborolimulus superspinosus gen. et sp. nov.	Austrolimulidae	Petropavlovka Formation, Cis-Urals, Russia	Early Triassic (Olenekian, ?Spathian)	Marginal marine to freshwater
Batracholimulus fuchsbergensis (Hauschke & Wilde, 1987)	Austrolimulidae	Exter Formation, Germany	Late Triassic (Rhaetian)	Marginal marine to freshwater
Dubbolimulus peetae Pickett, 1984	Austrolimulidae	Ballimore Formation, New South Wales, Australia	Middle Triassic (Ladinian)	Marginal marine to freshwater
Limulitella bronni (Schimper, 1853)	?Austrolimulidae	Grés á Voltzia Formation, France	Middle Triassic (Anisian)	Marginal marine to freshwater
Limulitella liasokeuperinus (Braun, 1860)	?Austrolimulidae	?Exter Formation-?Bayreuth Formation	Late Triassic-Early Jurassic (?Rhaetian- Hettangian)	Marginal marine to freshwater
Limulitella tejraensis Błażejowski, Niedźwiedzki, Boukhalfa & Soussi, 2017	?Austrolimulidae	Ouled Chebbi Formation, Tunisia	Middle Triassic (Anisian-Early Ladinian)	Marginal marine to freshwater
Limulitella volgensis Ponomarenko, 1985	?Austrolimulidae	Rybinsk Formation, Russia	Early Triassic (Olenekian)	Marine
Psammolimulus gottingensis Lange, 1923	Austrolimulidae	Solling Formation, Germany	Early Triassic (Olenekian, Spathian)	Marginal marine to freshwater
Vaderlimulus tricki Lerner, Lucas & Lockley, 2017	Austrolimulidae	Thaynes Group, Idaho, USA	Early Triassic (Olenekian, Spathian)	Marginal marine
Heterolimulus gadeai (Vía & Villalta, 1966)	Limulidae	Alcover Limestone Formation, Spain	Middle Triassic (Ladinian)	Marine
Keuperlimulis vicensis (Bleicher, 1897)	Limulidae	Keuper Formation, France	Late Triassic	Marine
Mesolimulus crespelli Vía Boada, 1987	Limulidae	Alcover Limestone Formation, Spain	Middle Triassic (Ladinian)	Marine
Sloveniolimulus rudkini Bicknell, Žalohar, Miklavc, Celarc, Križnar & Hitij, 2019	Limulidae	Strelovec Formation, Slovenia	Middle Triassic (Anisian)	Marine
Tarracolimulus rieki Romero & Vía Boada, 1977	Limulidae	Alcover Limestone Formation, Spain	Middle Triassic (Ladinian)	Marine
Yunnanolimulus (?) henkeli (von Fritsch, 1906)	Limulidae	Jena Formation, Germany	Middle Triassic (Anisian)	Marine
Yunnanolimulus luopingensis Zhang, Hu, Zhou, Iv & Bai, 2009	Limulidae	Guanling Formation, Luoping, China	Middle Triassic (Anisian)	Marine

585

586 **Table 1**: Summary of known Triassic xiphosurids. Taxa are order by family and then alphabetically by genus and species. Temporal
587 data taken from Bicknell & Pates (2020), Bicknell et al. (2020), Bicknell et al. (2021a), and Bicknell et al. (2021b). Note the uncertain
588 placement of *Limulitella* in Austrolimulidae, and *Yunnanolimulus henkeli*. In Figure 10 and Supplemental Information 3, *Limulitella* is
589 placed within Limulidae, and *Yunnanolimulus (?) henkeli* is referred to *Limulitella henkeli* (following Bicknell et al., 2021a).

Landmark number	Description of landmark
Landmark 1	Anterior-most prosomal point along sagittal line
Landmark 2	Distal-most prosomal point along sagittal line
Landmark 3	Posterior-most point of ophthalmic ridge
Landmark 4	Distal-most point of genal spine

590

591 **Supplementary Table 1:** Summary of digitised landmarks depicted in Figure 2.

592

Figure 1

Figure 1: Geographical and geological information for the studied fossil site.

(A) Map showing locality of Petropavlovka III (red star). (B) Stratigraphic log of Petropavlovka II–IV sections showing location of horseshoe crab-bearing lens (modified from Tverdokhlebov, 1967).

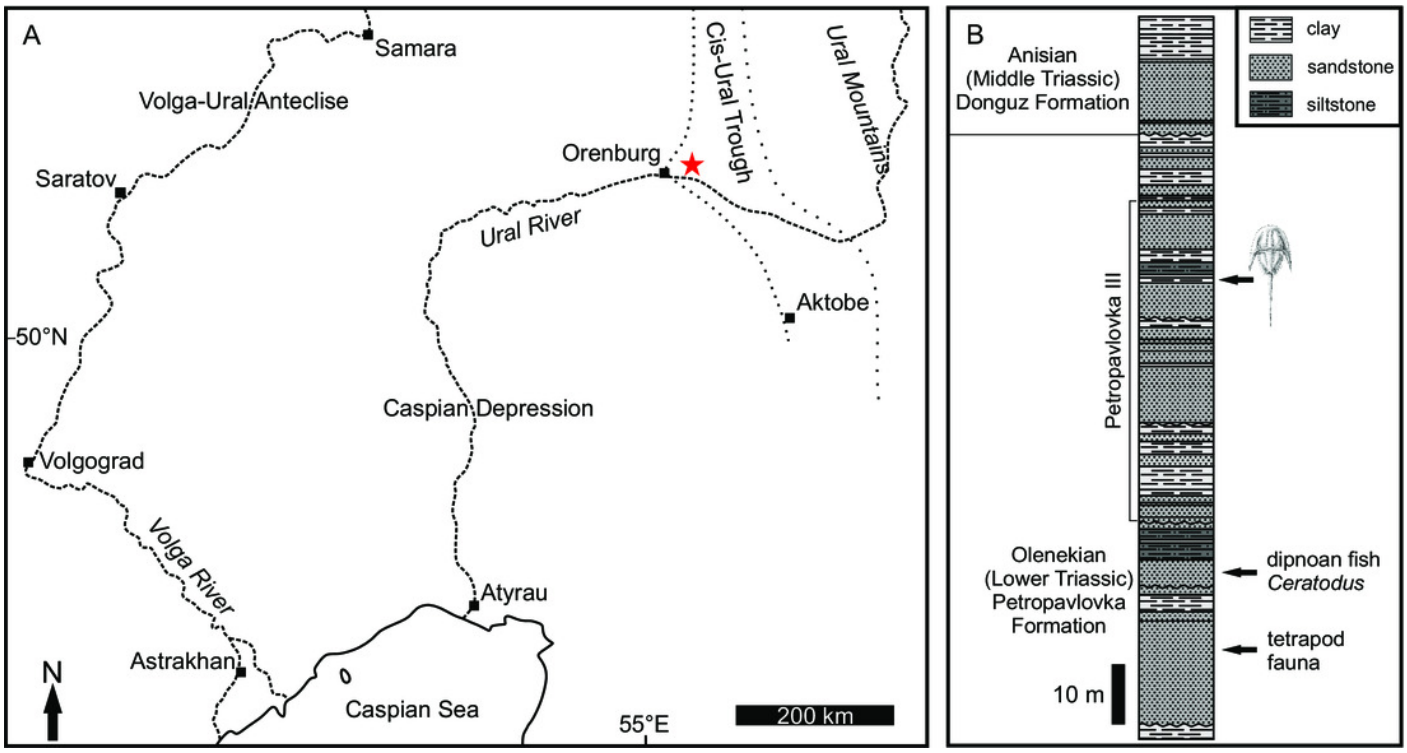

Figure 2

Depiction of geometric morphometric data gathered here: four landmarks and one semilandmark outline.

Consider Supplementary Table 1 for description of landmarks.

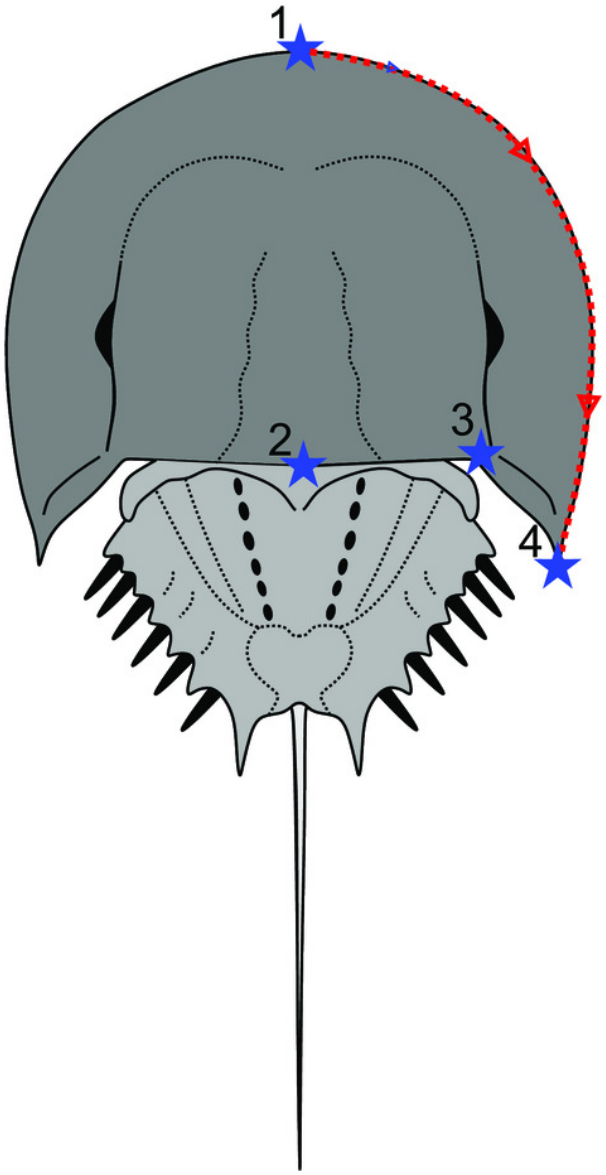
1
2
3
4

Figure 3

Holotype of *Attenborolimulus superspinosus* gen. et sp. nov. PIN 5640/220, counterpart.

(A, B): Photograph and interpretative drawing. Image credit: Sergey Bagirov. Abbreviations: Car: cardiac lobe; Eye: lateral compound eye; Fla: thoracetronic flange; Fs: fixed spine; Med: medial thoracetronic lobe; Oph: ophthalmic ridge; Pa: prosomal appendage; Pro: prosoma; Thr: thoracetron; Tel: telson.

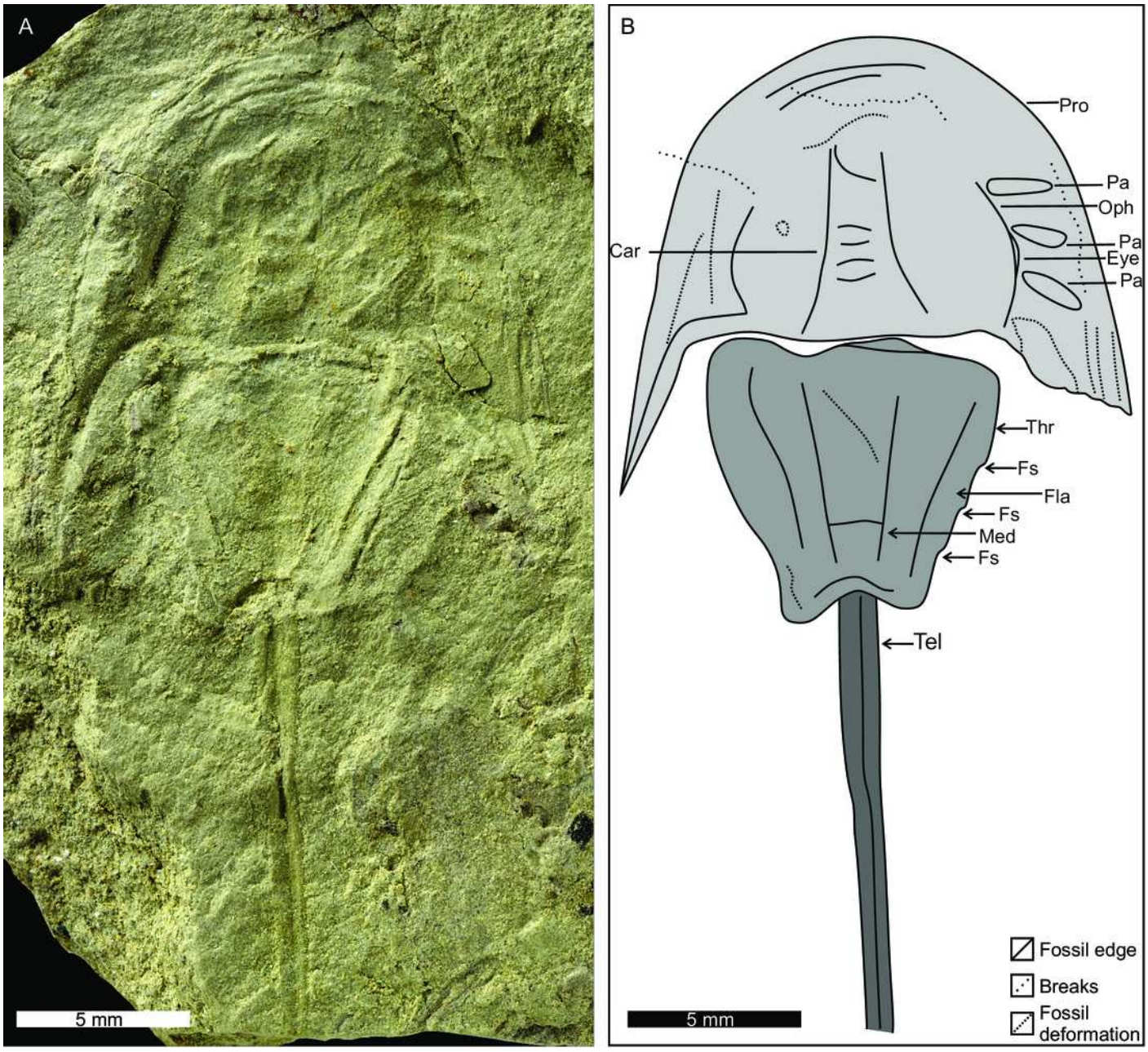
A
5 mm
B
Pro
Pa
Oph
Pa
Car
Eye
Pa
Thr
Fs
Fla
Fs
Med
Fs
Tel
5 mm
Fossil edge
Breaks
Fossil deformation

Figure 4

Holotype of *Attenborolimulus superspinosus* gen. et sp. nov., PIN 5640/220, part.

(A, B): Photograph and interpretative drawing. Image credit: Dmitry Shcherbakov.

Abbreviations: Car: cardiac lobe; Fla: thoracetronic flange; Med: medial thoracetronic lobe; Oph: ophthalmic ridge; Pa: prosomal appendage; Pro: prosoma; Thr: thoracetron; Tel: telson.

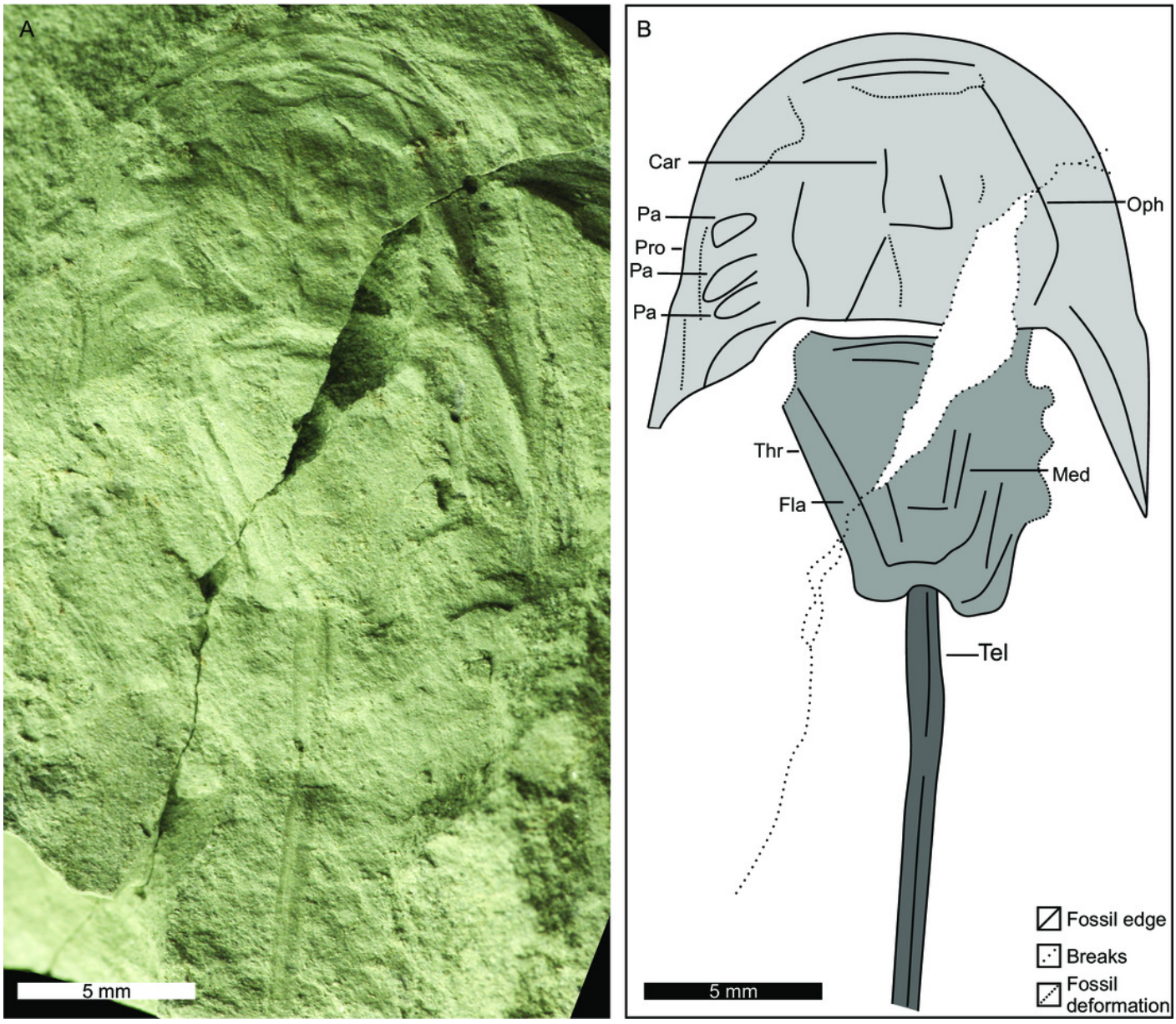

Figure 5

SEM images of the *Attenborolimulus superspinosus* gen. et sp. nov.

(A, C, D): Holotype, PIN 5640/220, counterpart. (A) Entire specimen. (C) Close up of box in (A), showing small moveable spine notches and fixed spines (white arrows). (D): Close up of box in (A), showing tubercles along prosomal thoracetronic border (white arrows). (B): Paratype, PIN 5640/200, part. Image credit: Dmitry Shcherbakov.

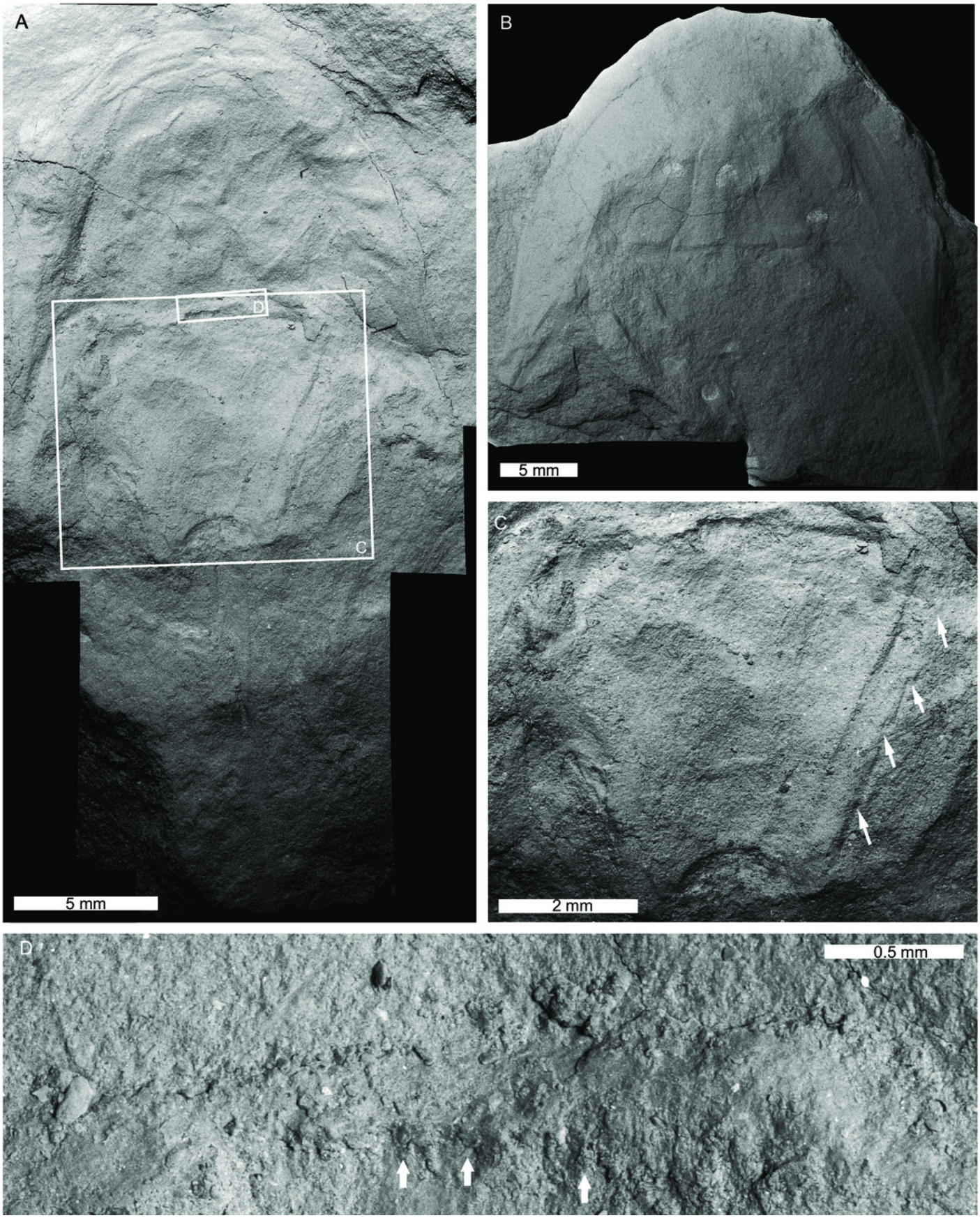
A
D
C
5 mm
B
5 mm
C
2 mm
D
0.5 mm

Figure 6

Paratype PIN 5640/200 of *Attenborolimulus superspinosus* gen. et sp. nov. showing key prosomal features.

(A, B): Part, photograph and interpretative drawing. (C, D): Counterpart, photograph and interpretative drawing. Image credit: Dmitry Shcherbakov. Abbreviations: Car: cardiac lobe.

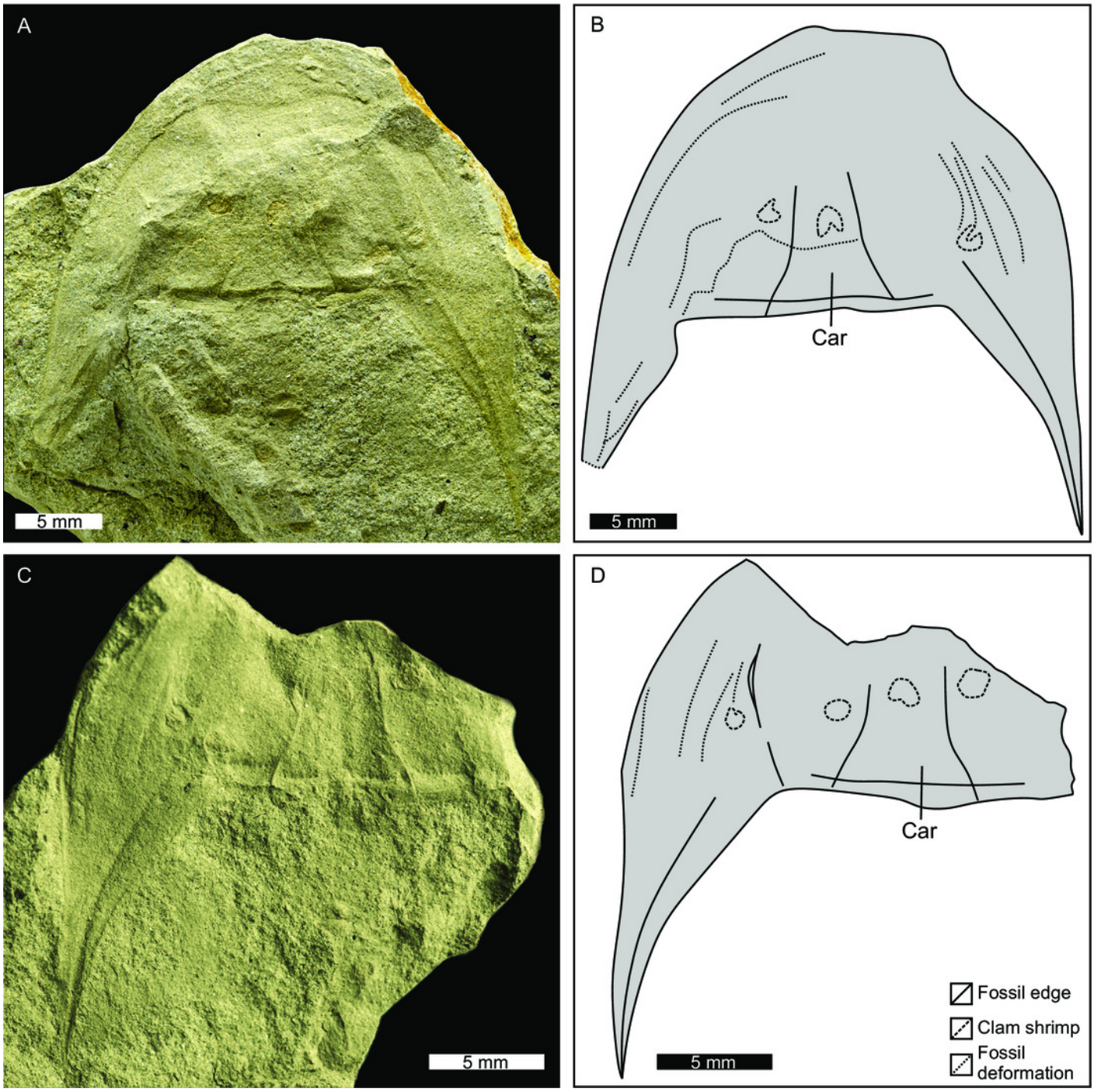
A
5 mm
B
Car
5 mm
C
5 mm
D
Car
5 mm
Fossil edge
Clam shrimp
Fossil deformation

Figure 7

Paratype PIN 5640/217 of *Attenborolimulus superspinosus* gen. et sp. nov.

(A, B): Photograph and interpretative drawing. Image credit: Sergey Bagirov.

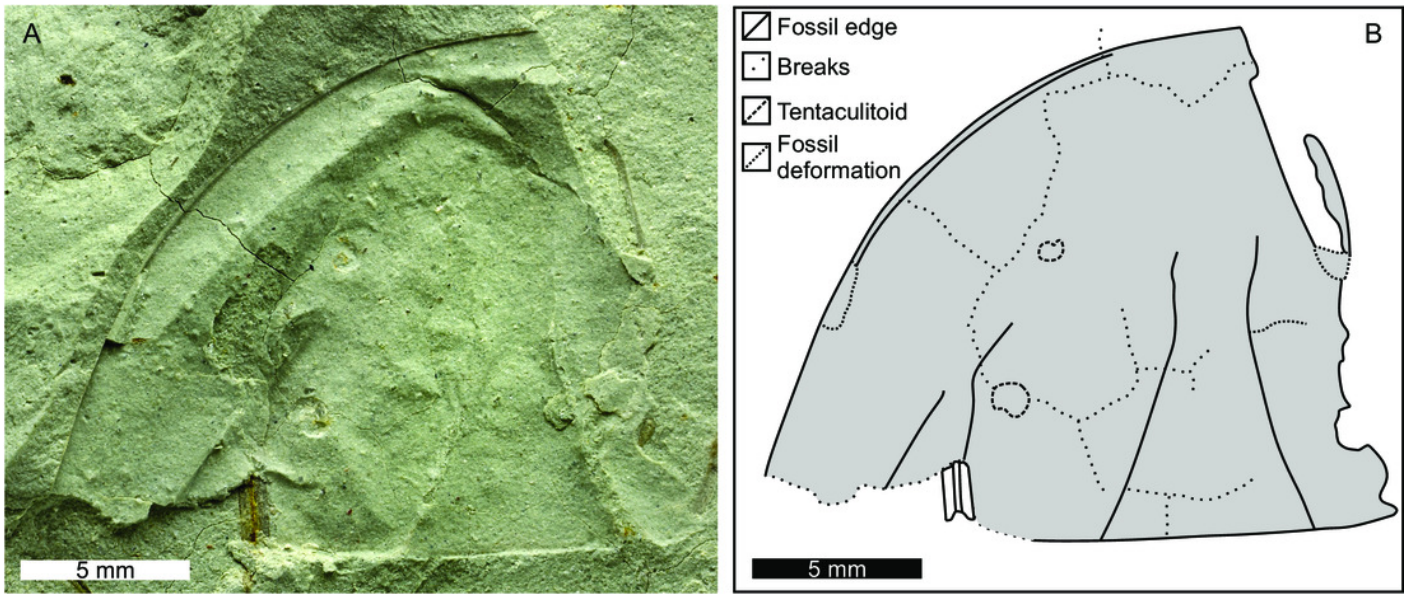

Figure 8

Figure 8. Reconstruction of *Attenborolimulus superspinosus* gen. et sp. nov.

Reconstruction credited to Katrina Kenny.

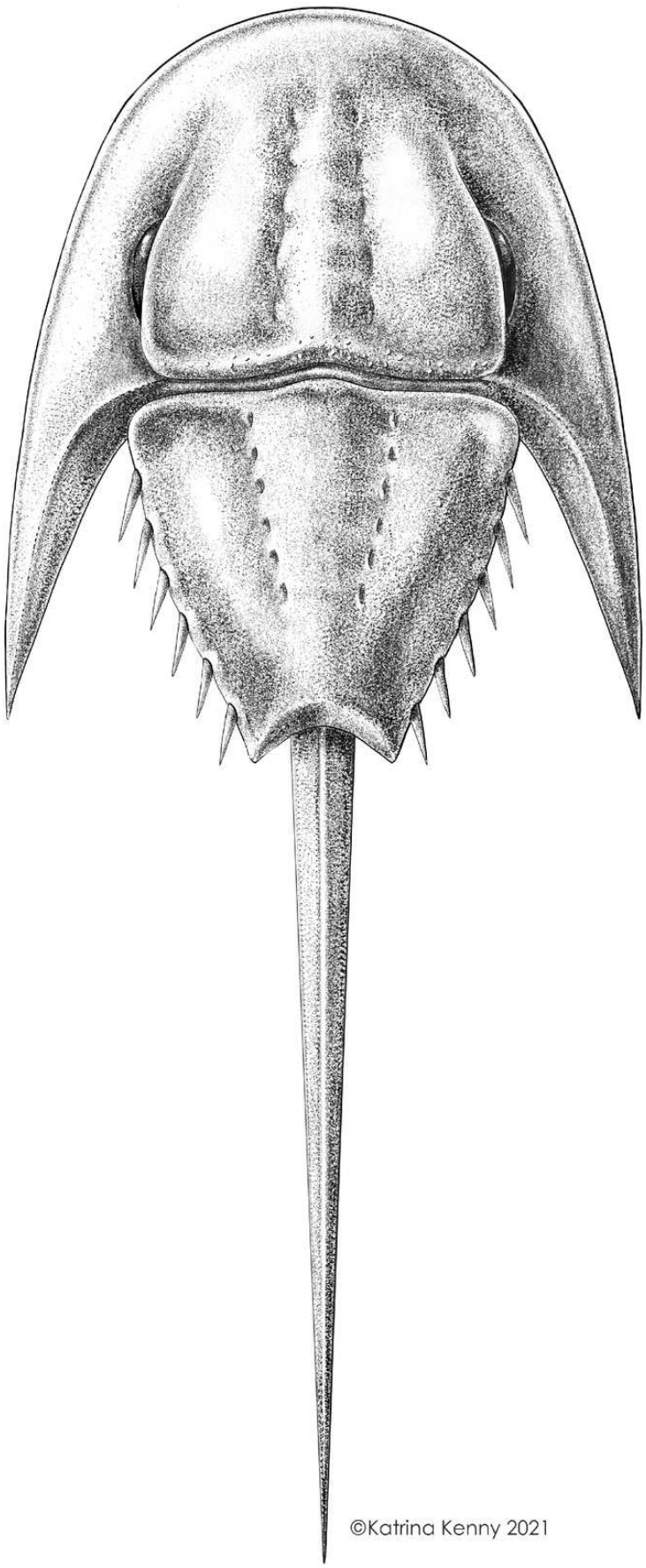
©Katrina Kenny 2021

Figure 9

Three examined xiphosurids families in PC space.

Austrolimulids occupy most positive PC1 space while limulids and paleolimulids are mostly constrained to negative PC1 space. *Attenborolimulus superspinosus* gen. et sp. nov. falls within the convex hull occupied by Austrolimulidae. Note that the austrolimulid morphospace excludes *Limulitella* specimens, as the position of this genus in Austrolimulidae is considered dubious.

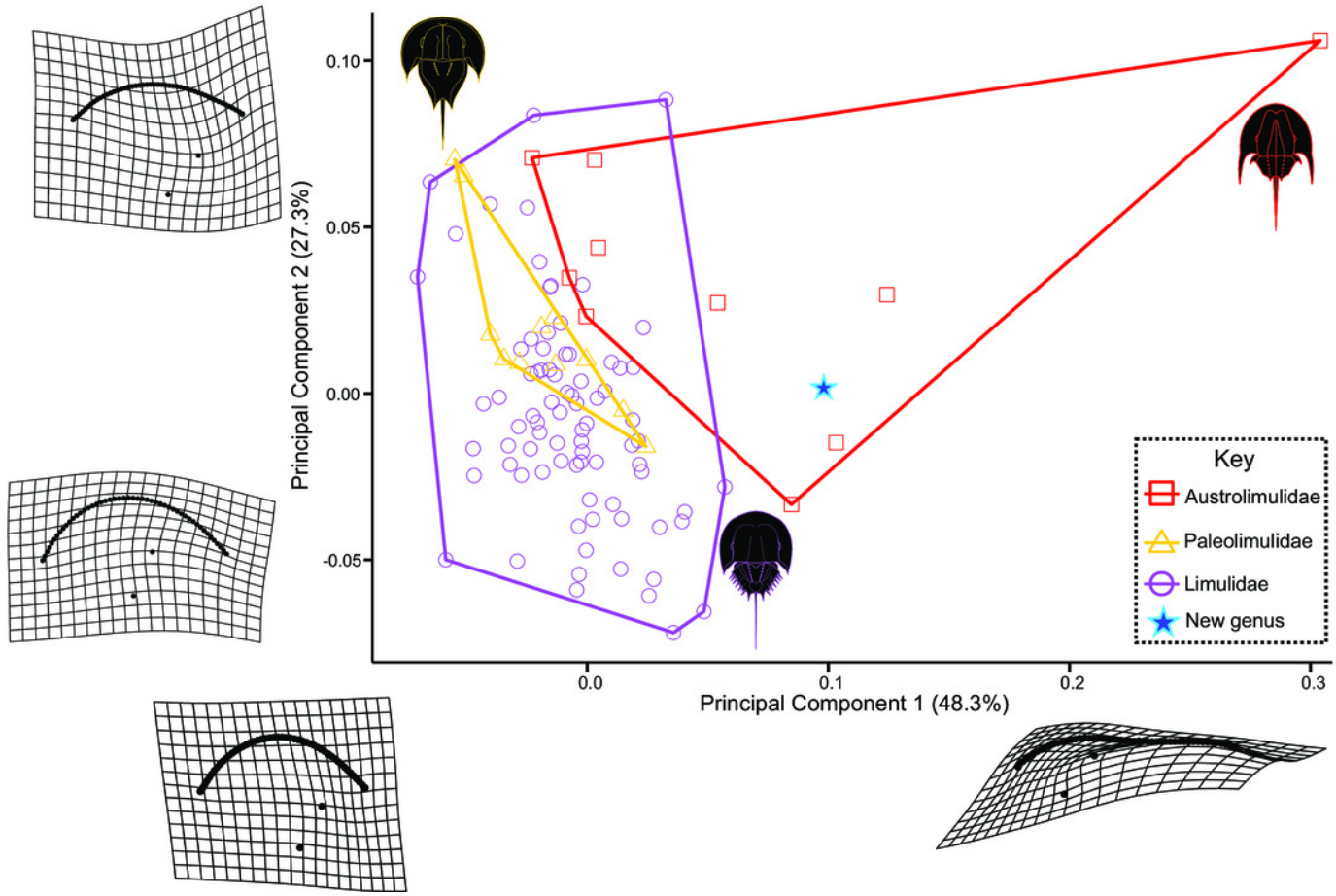
0.10
0.05
0.00
-0.05
Principal Component 2 (27.3%)
0.0
0.1
0.2
0.3
Principal Component 1 (48.3%)
Key
Austrolimulidae
Paleolimulidae
Limulidae
New genus

Figure 10

Figure 10. PC plot showing morphospace occupied by xiphosurid genera.

Where more than one specimen was digitised, genera are bound by convex hulls. *Attenborolimulus superspinosus* gen. et sp. nov. is not bound by any convex hull, excluding the specimen from other genera.

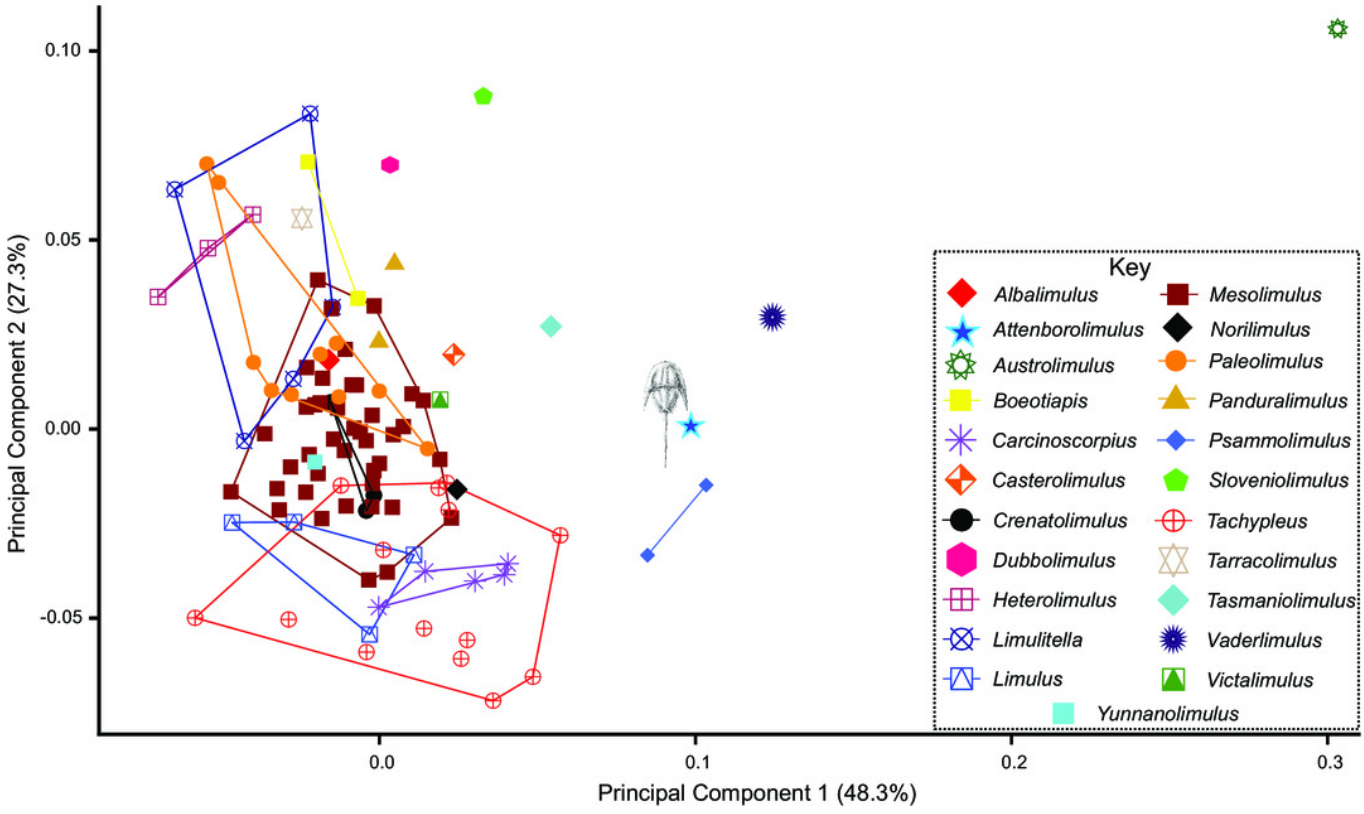
0.10
0.05
0.00
-0.05
Principal Component 2 (27.3%)
0.0
0.1
0.2
0.3
Principal Component 1 (48.3%)
Key
Albalimulus
Attenborolimulus
Austrolimulus
Boeotiapis
Carcinoscorpius
Casterolimulus
Crenatolimulus
Dubbolimulus
Heterolimulus
Limulitella
Limulus
Mesolimulus
Norilimulus
Paleolimulus
Panduralimulus
Psammolimulus
Sloveniolimulus
Tachypleus
Tarracolimulus
Tasmaniolimulus
Vaderlimulus
Victalimulus
Yunnanolimulus